Phase Diagram of Single Vesicle Dynamical States in Shear Flow

J. Deschamps, V. Kantsler, and V. Steinberg

Department of Physics of Complex Systems, Weizmann Institute of Science, Rehovot, 76100 Israel

(Received 30 October 2008; published 17 March 2009)

We report the first experimental phase diagram of vesicle dynamical states in a shear flow presented in a space of two dimensionless parameters suggested recently by V. Lebedev *et al.* To reduce errors in the control parameters, 3D geometrical reconstruction and determination of the viscosity contrast of a vesicle *in situ* in a plane Couette flow device prior to the experiment are developed. Our results are in accord with the theory predicting three distinctly separating regions of vesicle dynamical states in the plane of just two self-similar parameters.

DOI: 10.1103/PhysRevLett.102.118105 PACS numbers: 87.16.D−, 82.70.Uv, 83.50.−v

Understanding rheology of biofluids remains a great challenge and its progress is based on detail studies of dynamics of a single cell. Vesicle is a model system to study dynamical behavior of biological cells, and its dynamics in a shear flow was a subject of intensive theoretical [1–6], numerical [7–10] and experimental [11–16] research for the past decade.

A vesicle is a droplet of viscous fluid surrounded by a phospholipid bilayer membrane suspended in a fluid of either the same or different viscosity as the inner one. Both the volume and the surface area of the vesicle are conserved. The former means that the vesicle membrane is considered to be impermeable, at least on the time scale of the experiment, and the latter means that the membrane dilatation is neglected [1,2]. Already the first model of vesicle dynamics in a shear flow [17] reveals tank-treading (TT) and tumbling (TU) motions and transition between them, where the regions of existence of TT and TU depend on two control parameters: the excess area, $\Delta = A/R^2 - 4\pi$, and the viscosity contrast, $\lambda = \eta_{\text{in}}/\eta_{\text{out}}$. Here R is the effective vesicle radius related to its volume via $V = \frac{4}{3}\pi R^3$, A is the vesicle surface area, η_{in} and η_{out} are the dynamic viscosities of the inner and outer fluids, respectively. At sufficiently low $\lambda < \lambda_c(\Delta)$, a vesicle preserves θ, the inclination angle between its long axis and the shear flow direction, and its shape besides thermal fluctuations, while the membrane implements TT motion [1,7,12,13,17]. At $\lambda > \lambda_c(\Delta)$, according to theoretical predictions [2,17] and recent experiments [14], the transition to TU occurs, when a vesicle axis rotates with respect to the flow direction. It is remarkable that both TT and the transition line are independent of the shear rate, $\dot{\gamma}$, and described by a single equation for θ [1,17]. The next key observation is a new type of an unsteady motion, coined by us trembling (TR) [14]. This dynamical regime is distinguished by the inclination angle oscillation $|\theta(t)| < \pi/2$ around the flow direction accompanied by strong deformations of the vesicle shape. The latter is also revealed in the TU but in much less degree. A crucial aspect of TR is dependence of its existence region, which is separate from the TU region, on $\dot{\gamma}$. This is a distinct signature of the TR. Vesicle dynamics qualitatively similar to experimentally observed TR was independently predicted theoretically, though the distinctive feature was missing (there TR was coined as vacillating breathing mode coexisted with TU) [3]. The discovery of TR lead to reconsideration of the basic theoretical model. Recently three different theoretical models, which take into account coupling between the shape deformation and θ of a vesicle and dependence of TR dynamics on $\dot{\gamma}$, were suggested. They describe the regions of existence and transitions between TT, TR, and TU [5,10,18]. The qualitatively new result of the model presented in Ref. [5] is the self-similar solution obtained at $\Delta \ll 1$, which reduces five parameters in the problem, namely η_{out}, λ, $\dot{\gamma}$, R and Δ, just to two dimensionless ones [5]:

$$S = \frac{7\pi}{3\sqrt{3}} \frac{\dot{\gamma}\eta_{\text{out}} R^3}{\kappa\Delta}, \tag{1}$$

$$\Lambda = \frac{4}{\sqrt{30\pi}}\left(1 + \frac{23}{32}\lambda\right)\sqrt{\Delta}, \tag{2}$$

where κ is the bending modulus. It means that all vesicles with different geometrical characteristics, R and Δ, can be presented on the 2D phase diagram, contrary to the 3D phase diagrams suggested in Ref. [10] with Δ as the third parameter. On the other hand, the authors of Ref. [18] claim that a hydrodynamic response of the the next order term in the Helfrich force, which is significant and breaks the self-similarity, is not taking into account in Ref. [5]. However, the additional terms suggested in Ref. [18] compared with Ref. [5] are of the next order in $\sqrt{\Delta}$ in the equation for the shape deformation parameter and of the same order in the equation for θ. It means that theory of Ref. [18] suggests a significant correction even for TT compared with the older [1,2,7,17] and recent theories [6] that are rather well established and tested by the experiment [13].

To test these theories and verify, which of them proper describe experimental data, significant improvement of the existing techniques of vesicle characterization and control of $\dot{\gamma}$ is required. Indeed, the determination of R and Δ of a 3D object extrapolated from a 2D vesicle contour leads up to about 20% error. The deviation of λ in each vesicle from

the value obtained during the preparation could also reach 20% or more. Besides theory considers pure 2D shear flow, whereas the previous experiments have been performed in a micro-channel flow with 8% deviation of $\dot{\gamma}$ from a constant value and another 5% due to vesicle sedimentation that caused a deviation from the shear plane into the third dimension. Thus the overall error in S could reach up to 100% and in Λ up to 35% that undermines a possibility of the experimental test of the phase diagram.

In this Letter we report the first experimental results on the phase diagram of the vesicle dynamical states, TT, TR, and TU, in a plane shear flow presented in the S and Λ self-similar parameters. It was accomplished due to the three technical achievements: (i) use of a plane Couette apparatus providing pure shear flow; (ii) 3D geometrical characterization of a vesicle *in situ* that reduces an error down to 3.5% in R and less than 16% in Δ; (iii) determination of λ *in situ* with an error of less than 1%. Thus altogether the errors were reduced down to about 25% in S and 8% in Λ.

Measurements of the vesicle dynamics were conducted in a plane Couette flow apparatus mounted on top of the inverted epifluorescent microscope. The device, similar to one described in Ref. [19], includes two parallel microscope cover glasses separated by a Teflon spacer to maintain a constant gap, $d = 111$ μm, and sliding on a coverslip (Fig. 1). One cover glass is driven by the computer-controlled close-loop, high resolution linear DC-Mike actuator (M-230.10, PI, Germany) coupled via a pulley to the second cover glass to bring it into relative motion. Particle tracking measurements of the velocity field show that the deviation of the measured $\dot{\gamma}$ from the expected $\dot{\gamma}_e = 2V/d$ is $<4\%$ with overall error in $\dot{\gamma}$ much below 4% (and mostly at low $\dot{\gamma}$) (Fig. 2). Observation of a vesicle was carried out above ~ 60 μm, where $\dot{\gamma}$ saturated (Fig. 2). The observation area 90×69 μm^2 was captured by Mintron MTV-12V6HC CCD camera and digitized via Ellips Rio frame grabber. A mechanical chopper was synchronized with the frame grabber decreasing the exposure time to reduce photobleaching.

Vesicles were prepared by electro-formation method [20]. We used a lipid solution consisted of 85% DOPC (Sigma) and 15% NBD-PC (fluorescent lipid, Molecular Probes) dissolved in 9:1 v/v chloroform-methanol solvent (1.8 mg/ml total lipid/ml), as described before [13]. As an inner fluid, a glucose-water solution with Mw = 500 kDa dextran in various proportions to adjust the fluid viscosity, was used. The viscosity contrast different from unity was achieved by using a sucrose-glucose-dextran-water solution with different sucrose concentration to equilibrate osmolarity and density and to control an outer fluid viscosity. The rheological measurements were carried out on a viscometer Vilastic-3. To reduce an error in λ, we measured the sedimentation velocity, V_{sed}, of each vesicle in the Couette flow device *in situ* prior to experiments. It was related to the difference between the inner ρ_{in} and outer ρ_{out} densities of fluids. We considered a vesicle as a hard ellipsoid of effective radius R_e, which was the function of three ellipsoid axes [21], moving under gravity in a viscous flow $\rho_{\mathrm{in}} - \rho_{\mathrm{out}} = \frac{9}{2}\frac{\eta_{\mathrm{out}} V_{\mathrm{sed}}}{g R_e^2}$. Then by using a relation $\lambda = f(\rho_{\mathrm{in}} - \rho_{\mathrm{out}})$ one obtained the expression for the viscosity contrast: $\lambda = F(V_{\mathrm{sed}})$. Applying this expression for each vesicle, we found variations up to 8% from the expected λ in the range from 1 to 7.5.

Another new aspect of this study was a 3D reconstruction *in situ* of a shape of each vesicle that provided precise values of its R and Δ. To conduct the measurement a vesicle during either the TT or TU at low $\dot{\gamma}$ was observed using an objective Zeiss Acroplan 63X. The vesicle was scanned by displacing the objective by a step of 1 μm. The scan was sufficiently fast ($<2s$) compared to the vesicle dynamics to avoid any large fluctuations in a size and a position of the vesicle [Fig. 3(a)]. Ellipses arisen from a fit of each slice were then stacked according to their heights with correction of the position of each slice on V_{sed} and the displacement in the (x, y) plane during the motion [Fig. 3(b)]. R and Δ were obtained from the fit by 3D ellipsoid. Thus, R varied from 4.5 μm up to 14 μm with

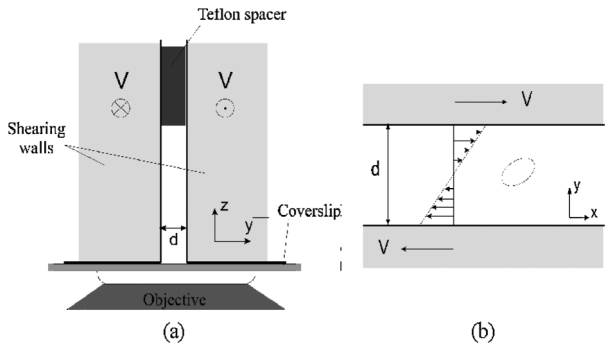

FIG. 1. Schematics of the plane Couette shear flow device. (a) side view. (b) view from below, from the objective side.

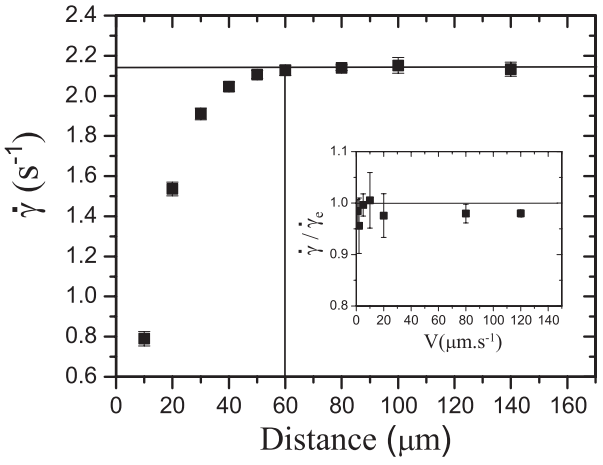

FIG. 2. Calibration plot of Couette flow for $V = 120$ μm $\cdot$ s^{-1} gives $\dot{\gamma} = 2.138 \pm 0.010$ s^{-1} versus $\dot{\gamma}_e = 2.152$ s^{-1}. Inset: $\dot{\gamma}/\dot{\gamma}_e$ versus velocity.

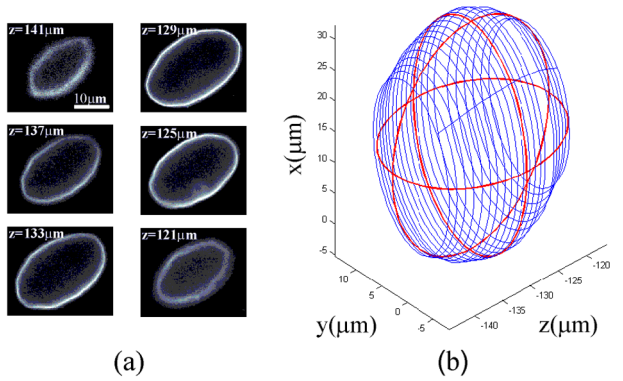

FIG. 3 (color online). Reconstruction of vesicle ellipsoidal shape. (a) several slices captured at different z. (b) elliptical approximation of each slice and their stacking in 3D space. Ellipsoidal approximation of 3D vesicle shape provides its three main axis. Here $R = 14.56 \pm 0.31$ μm and $\Delta = 0.49 \pm 0.04$.

an error of about 3.5%, while Δ varied in the range [0.2, 2.2] with an error less than 16%.

The experiments on vesicle dynamics were performed in two steps. First, a full characterization of a vesicle was fulfilled, namely, the 3D reconstruction of the vesicle shape and the measurement of λ. Second, the same vesicle was followed at a required $\dot{\gamma}$ and a given λ in a moving frame. To explore the whole space of parameters (S, Λ), $\dot{\gamma}$ was varied to scan the phase diagram horizontally. The various types of motions were distinguished in the following way. A captured vesicle was fitted by an ellipse in each time step, and the motion of its major axis was analyzed as a function of time: TU corresponds to a complete reversal of the major axis, TR is defined by variation of θ less than $\pi/2$, and TT was found, if θ was rather constant (Fig. 4). In Fig. 5 we present an example of the transition from the TU to TR motions of the same vesicle due to variations in $\dot{\gamma}$ characterized by its θ and the aspect ratio D time dependence.

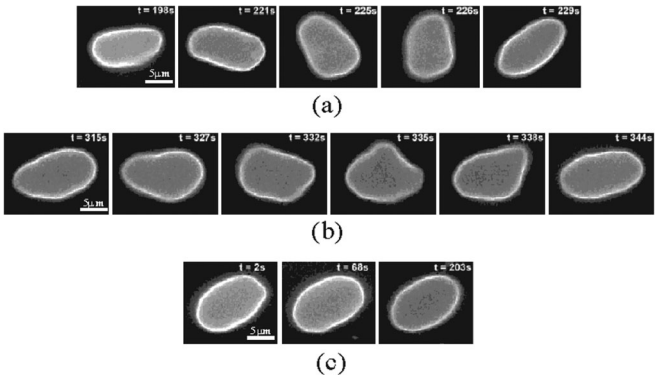

FIG. 4. Dynamical states of vesicles. (a) TU: $R = 5.9 \pm 0.1$ μm, $\Delta = 0.82 \pm 0.11$, $\dot{\gamma} = 0.40$ s^{-1} and $\eta_{in}/\eta_{out} = 6.12$; (b) TR: $R = 5.44 \pm 0.13$ μm, $\Delta = 0.84 \pm 0.09$, $\dot{\gamma} = 0.80$ s^{-1} and $\eta_{in}/\eta_{out} = 6.11$ (c) TT: $R = 6.17 \pm 0.02$ μm, $\Delta = 0.68 \pm 0.05$, $\dot{\gamma} = 0.13$ s^{-1} and $\eta_{in}/\eta_{out} = 1$

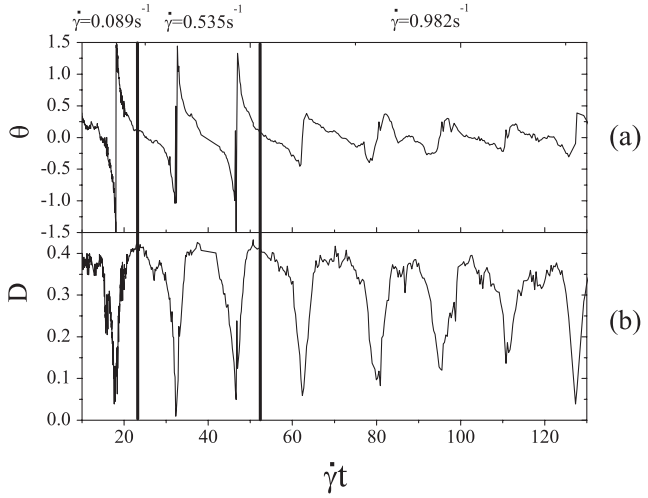

FIG. 5. Transition from TU to TR due to $\dot{\gamma}$ variations. (a) θ and (b) $D = \frac{L-B}{L+B}$ versus normalized time. L and B are the large and small semiaxis of the vesicle elliptical approximation. $\Delta = 0.99$, $R = 6.89$ μm, $\lambda = 6.25$

In Fig. 6 we present the experimental data of different dynamical regimes on the S, Λ-plane. The grey bands separate regions with different dynamics. The theoretically predicted lines separating TT from TU and TR, and TR from TU taken from Ref. [5] are also shown.

The main conclusion from the experimental phase diagram is that TT, TU and TR are separated into three regions in S and Λ variables for the wide range of the physical parameters with Δ distributed rather randomly across the plane. The independence of the location of the different dynamical states of the vesicle on Δ in a wide range of S, Λ

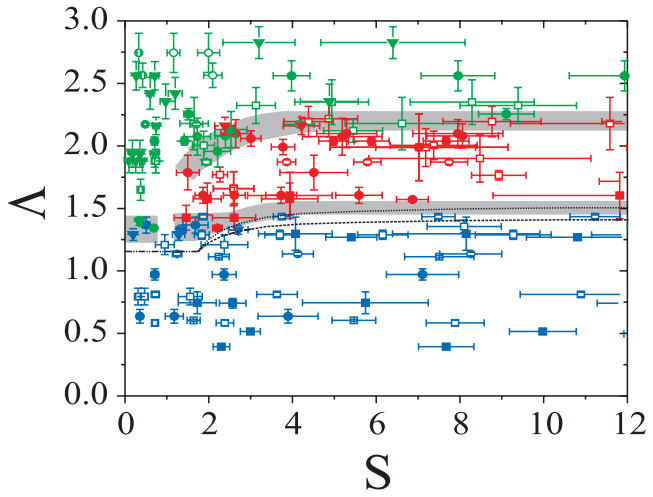

FIG. 6 (color). Phase diagram of the vesicle dynamical states in a shear flow: blue symbols—TU, red—TR, black—TT. ■—△∈ [0–0.55], □—△∈ [0.55–0.8], ●—△∈ [0.8–1.05], ○—△∈ [1.05–1.25], ▼—△∈ [1.25–2]. Gray bands are guides for the eye. Dotted, dashed, and solid black lines are the theoretical boundaries between TT, TU, and TR, respectively.

and Δ points out on the self-similarity in the vesicle dynamics suggested in Ref. [5], despite of the fact that the theory is developed for $\Delta \ll 1$, whereas in the experiment vesicles are in the range $0.2 \leq \Delta \leq 2.2$. On the other hand, the authors of Ref. [18] applied their theory for $\Delta = 1$, where the deviation from the self-similarity should be of order $O(1)$ and observable experimentally. These facts and arguments provide a basis to state that two models suggested in Refs. [10,18], are not consistent with the experiment.

It is also noticeable that the experimental data show qualitatively the same topological structure of the phase diagram as in Ref. [5]; i.e., the lines separating TT, TR, and TU regions have the same structure. However the experimental TR region is considerably wider than the theoretical one and globally shifted slightly up in Λ and left in S. These discrepancies could have several causes. First, we mostly observed vesicles with large Δ, whereas the theory was developed for $\Delta \ll 1$. Second, thermal noise was not taking into account within the theory [5]. Moreover, the description of the vesicle TU and TR dynamics was done up to the second harmonic only (elliptical shape deformations). Though this approach works well for the TT motion, the deviation from the elliptical shape and the higher order modes are involved in the dynamics of TU and particularly of TR [see Fig. 4(b)]. Here we would like to emphasize that contrary to TT in TU and TR a vesicle is subjected to periodical stretching and compression, which lead to its shape deformations like in a time-dependent elongation flow studied recently [16]. Because of the volume and surface area conservations, strong shape deformations can occur mostly via a concavity, which is indeed observed during TR cycle [see Fig. 4(b)] and is associated with a negative surface tension. This scenario and deformed vesicle shapes with clear signature of the third and even higher harmonics in TR in Fig. 4(b) could be the main reason for the discrepancy in the width of the TR region. The vesicle shape deformations in TR also distinctly differ from those shown in snapshots of the vacillating breathing mode in [18], where they are remained of elliptical shape and indeed imitate breathing, whereas in the experiment they look more like trembling.

We also point out the fact that exploring the vicinity of the critical point ($S \simeq 1.8$ and $\Lambda \simeq 1.18$), which according to the theory has a very complicated structure, is not feasible due to limited resolution in the determination of S and Λ.

To conclude, we developed new experimental methods to obtain the first experimental diagram of the vesicle dynamics in a plane shear flow. The plane Couette shear flow allows to observe a vesicle at a constant $\dot{\gamma}$ for a long time. Reconstruction of a 3D vesicle shape, that provides Δ and R, and determination of λ *in situ* in the same device drastically reduce the experimental error in S and Λ. The experimental results are in a good qualitative agreement with the theory [5] showing distinct separation of the vesicle dynamical states on the 2D phase diagram in S and Λ variables and the self-similar solution is valid, though the theory was developed for $\Delta \ll 1$ and by neglecting thermal noise, whereas vesicles with $\Delta \sim O(1)$ were observed in the experiment. But in the light of the arguments in Ref. [18], the puzzle remains: what is the reason for prevailing of the self-similar solution up to $\Delta \sim O(1)$?

We thank V. Lebedev and N. Zabusky for helpful remarks and suggestions and E. Segre for help in software support. This work is partially supported by grants from Israel Science Foundation, the Minerva Foundation, the Israeli Ministry of Science, Culture & Sport for Russian-Israeli Cooperation, and by the Minerva Center for Nonlinear Physics of Complex Systems.

[1] U. Seifert, Eur. Phys. J. B **8**, 405 (1999).
[2] F. Rioual, T. Biben, and C. Misbah, Phys. Rev. E **69**, 061914 (2004).
[3] C. Misbah, Phys. Rev. Lett. **96**, 028104 (2006).
[4] P. Vlahovska and R. Gracia, Phys. Rev. E **75**, 016313 (2007).
[5] V. V. Lebedev, K. S. Turitsyn, and S. S. Vergeles, Phys. Rev. Lett. **99**, 218101 (2007); New J. Phys. **10**, 043044 (2008).
[6] R. Finken, A. Lamura, U. Seifert, and G. Gompper, Eur. Phys. J. E **25**, 309 (2008).
[7] J. Beaucourt *et al.*, Phys. Rev. E **69**, 011906 (2004).
[8] H. Noguchi and G. Gompper, Phys. Rev. Lett. **93**, 258102 (2004).
[9] H. Noguchi and G. Gompper, Phys. Rev. E **72**, 011901 (2005).
[10] H. Noguchi and G. Gompper, Phys. Rev. Lett. **98**, 128103 (2007).
[11] K. de Haas *et al.*, Phys. Rev. E **56**, 7132 (1997).
[12] M. Abkarian, C. Lartigue, and A. Viallat, Phys. Rev. Lett. **88**, 068103 (2002).
[13] V. Kantsler and V. Steinberg, Phys. Rev. Lett. **95**, 258101 (2005).
[14] V. Kantsler and V. Steinberg, Phys. Rev. Lett. **96**, 036001 (2006).
[15] M. A. Mader *et al.*, Eur. Phys. J. E **19**, 389 (2006).
[16] V. Kantsler, E. Segre, and V. Steinberg, Phys. Rev. Lett. **99**, 178102 (2007).
[17] S. R. Keller and R. Skalak, J. Fluid Mech. **120**, 27 (1982).
[18] G. Danker *et al.*, Phys. Rev. E **76**, 041905 (2007).
[19] R. E. Teixeira, H. P. Babcock, E. S. G. Shaqfeh, and S. Chu, Macromolecules **38**, 581 (2005).
[20] M. I. Angelova *et al.*, Prog. Colloid Polym. Sci. **89**, 127 (1992).
[21] J. Happel and H. Brenner, *Low Reynolds Number Hydrodynamics* (Springer, New York, 1987).